Analytical Methods

Differential analysis of phytochemistry and antioxidant activity in five citrus by-products based on chromatography, mass spectrometry, and spectrum-effect relationships

Jiangyi Luo, Ling Liang, Qinling Xie, Yixing Qiu, Sai Jiang, Yupei Yang, Lijuan Zhu, Yangfen Fu, Shenghuang Chen, Wei Wang [*], Hanwen Yuan [*]

TCM and Ethnomedicine Innovation & Development International Laboratory, Innovative Material Medical Research Institute, School of Pharmacy, Hunan University of Chinese Medicine, Changsha, China

ARTICLE INFO

ABSTRACT

The unripe fruit or peel of *Citrus aurantium* L., *Citrus sinensis* Osbeck, and *Citrus reticulata* Blanco are often disregarded due to perceptions of their marginal value. The present study was undertaken to explore the differences in phytochemical composition and bioactive properties of five citrus by-products in China and demonstrate their potential value. 214 compounds were systematically identified using LC-Orbitrap-MS analysis. Among them, narirutin, naringin, hesperidin, and neohesperidin were established as essential compounds for the discrimination and authentication of the five by-products via a combination of LC-MS, HPLC, and TLC techniques. Variations in the antioxidant activity of the by-products were observed, which correlated with their maturity and were attributable to differences in their active ingredients. Moreover, spectrum-effect relationship analysis revealed that the four previously identified differential markers, along with nobiletin and tangeretin, significantly contributed to the differences in antioxidant activity. The results highlight the potential for citrus by-product enhancement and utilization.

1. Introduction

Citrus fruits, such as sour or bitter oranges (*C. aurantium*), sweet oranges (*C. sinensis*), and mandarin oranges (*C. reticulata*) (Tocmo, Pena-Fronteras, Calumba, Mendoza, & Johnson, 2020), are of considerable agronomic importance, with a global yield attaining 135.9 million tonnes in 2017 (B. Singh, Singh, Kaur, & Yadav, 2021). The mature fruits of *C. sinensis* and *C. reticulata* are consumed fresh worldwide owing to their optimal sugar-to-acid ratio, aromatic qualities, and juicy pulp (Zhao et al., 2019). Conversely, the distinctive pungent acidity of *C. aurantium* fruits predisposes their use predominantly in beverages, canned products, or as flavoring agents (Farag, Abib, Ayad, & Khattab, 2020). Various factors throughout the growth cycle may result in premature fruit drop, leading to the disposal of young or immature fruits. Similarly, citrus peels are commonly discarded, contributing to substantial environmental concerns worldwide, with estimates indicating an annual waste range of 8 to 20 million tonnes (Costanzo et al., 2022).

The concept of bioactive by-products and functional foods has prompted the emergence of products rich in unripe fruits or peels (Czech, Malik, Sosnowska, & Domaradzki, 2021). In China, the utilization of these products extends beyond millennia, with current recognition as dietary herbal medicine or health foods (Jiangyi Luo et al., 2023). Suancheng Zhishi (SCZS), harvested between May and June as the young fruit of *C. aurantium* or its most common Daidai cultivar (Yu et al., 2020), and Zhiqiao (ZQ), collected as the immature fruit in July, are notable examples. Qingpi (QP) is derived from the young fruits of *C. reticulata* between May and June or from the peels of immature fruits between July and August, whereas Chenpi (CP) is prepared from the peels of mature fruits (Commission, 2020). More recently, Tiancheng Zhishi (TCZS) from the young fruits of *C. sinensis* has garnered extensive popularity (Xie, 1991). These dried products are highly effective at promoting expectoration and enhancing gastrointestinal motility, offering substantial benefits for digestion and bowel movements (Liang et al., 2022). Interestingly, citrus by-products have been regarded as a superior source of antioxidants, surpassing fruit pulp (Czech et al., 2021). Noteworthily, the consumption of food high in antioxidants may aid in a reduction in the incidence of chronic degenerative diseases, which are linked to oxidative stress (Costanzo et al., 2022).

J. Luo et al. *Food Chemistry: X 20 (2023) 101010*

The composition and therapeutic effects of these by-products vary with their degree of maturity (Tang et al., 2021). Nevertheless, the proximity of their harvest times and similar appearances can lead to frequent mixed-use. Furthermore, previous research comparing several citrus fruits largely focused on fresh fruits, with limited scrutiny of young or immature fruits. Intriguingly, studies examining diverse citrus by-products, including the peel, pith, endocarp, and seed, have reported an abundance of flavonoids in the peel, alongside a remarkable anti-oxidant capacity (Sun, Wang, Gu, Liu, Zhang, & Zhang, 2010; Y. Wang et al., 2017). Detailed compositional and bioactivity analyses are indispensable to fully leverage the potential health benefits of their products.

In this study, liquid chromatography coupled with electrostatic Orbitrap high-resolution mass spectrometry (LC-Orbitrap-MS) identified 214 compounds. Hesperidin, neohesperidin, narirutin, and naringin were validated as key markers via LC-Orbitrap-MS, HPLC, and TLC for distinguishing between the five by-products. In addition, a spectrum-effect relationship study exposed significant variations in the DPPH (1,1-diphenyl-2-picryl-hydrazyl) and ABTS (2,2'-azino-bis(3-ethyl-benzothiazoline-6-sulphonic acid)) scavenging abilities among the products. The four differential markers identified, along with two polymethoxyflavones (nobiletin and tangeretin), emerged as influential compounds responsible for the discrepancies in antioxidant activity. Therefore, these six compounds exhibit potential as quality control markers.

Earlier studies primarily relied on a single chromatographic approach (Duan, Guo, Liu, Liu, & Li, 2014; Tian et al., 2020). In contrast, the current research comprehensively utilized multiple chromatographic techniques. Moreover, differential markers were initially screened from the full compositional spectrum via LC-MS, followed by validation using HPLC and TLC, resulting in more scientifically reliable outcomes and a more practical methodology. Therefore, this study is of paramount importance and practical value for the quality control and authentication of citrus by-products.

2. Materials and methods

2.1. Reagents and materials

Naringin, neohesperidin, nobiletin, and tangeretin were procured from NatureStandard (Shanghai, China). Hesperidin and synephrine were obtained from Baoji Herbest Bio-Tech (Baoji, China) and narirutin from Yuanye (Shanghai, China). MS-grade acetonitrile was obtained from Supelco (Burlington, MA, USA), and HPLC-grade methanol and acetonitrile from Sigma-Aldrich (Louis, USA). Analytical-grade reagents, including methanol, ethanol, acetone, anhydrous aluminum chloride, and formic acid, were sourced from Sinopharm (Shanghai, China). Deionized water was supplied by C'estbon (Changsha, China). The polyamide film plate was acquired from Sijia Biochem (Taizhou, China). The ABTS test kit was provided by Jiancheng Lab (Nanjing, China), and the DPPH reagent by Solarbio (Beijing, China).

Seventy-two sample batches, including 30 batches of SCZS, 5 of TCZS, 13 of ZQ, 12 of QP, and 12 of CP, were collected from 21 different regions across China. Details regarding the plant samples used in the experiments are delineated in Fig. 1 and Table S1.

2.2. Sample preparation

The samples were pulverized and sifted through a 50-mesh sieve. 0.5 g of powdered sample was added to 50 mL of methanol, followed by ultrasonic extraction for 45 min. The resulting solution was then centrifuged at 13,000 rpm for 10 min to obtain the test solution for HPLC and antioxidant activity analyses. Regarding LC-MS and TLC analyses, 0.2 g and 0.1 g of the sample were ultrasonically extracted with 20 mL and 10 mL of methanol for 30 min, respectively.

2.3. UPLC-MS analysis

The LC procedure utilized a Vanquish system equipped with a Hypersil GOLD^{TM} Aq-C$_{18}$ column (100 × 2.1 mm, 1.9 μm) (Thermo Scientific, MA, USA). The elution gradient consisted of 0.01 % formic acid water (A) and acetonitrile (B) in the following proportions: 0–2-4–7-10–15-17–18-23 min; 10–18-19–20-35–50-65–95-95 % B. The column temperature, flow rate, and injection volume were optimized to 35 °C, 0.3 mL/min, and 4 μL, respectively.

Mass spectrometric analysis was conducted using an Orbitrap Exploris 120 instrument in positive ion mode, offering a resolution of 60,000 across an m/z range of 100–1000 Da, and MS^2 was 15,000. Collision energies were set at 30 % for higher-energy collisional dissociation (HCD), with an ion spray voltage maintained at 3.5 kV. Gas flows for sheath, auxiliary, and sweep gases were set at 50, 10, and 1 Arb, respectively. The ion transfer tube and vaporizer temperatures were set
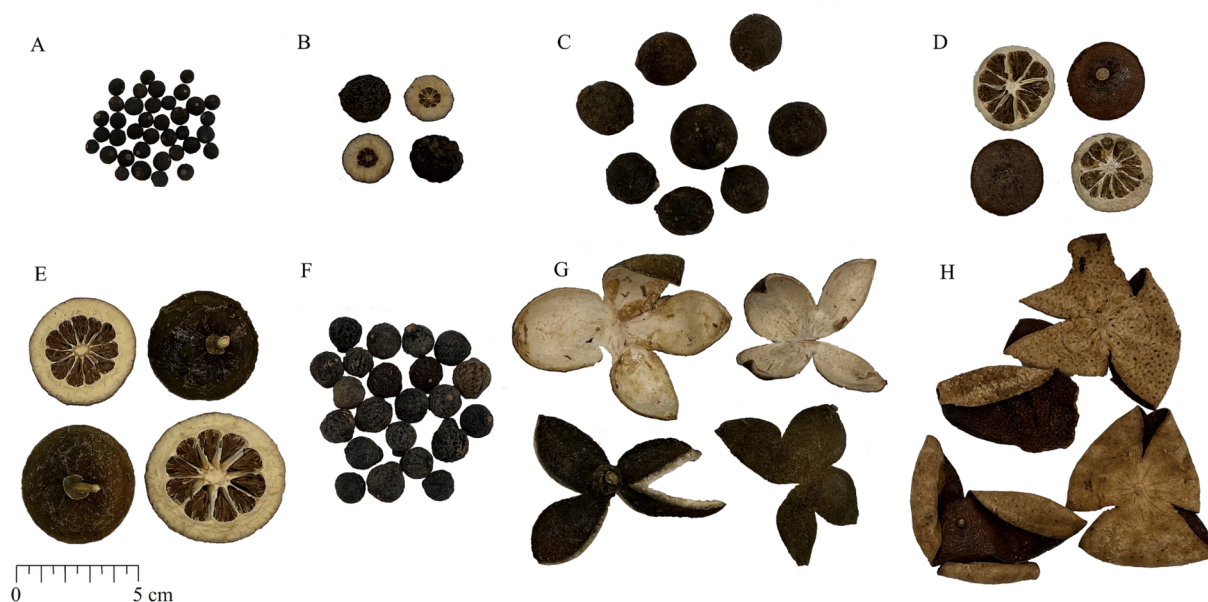

Fig. 1. Appearance of the collected sample (A-C: SCZS, D: TCZS, E: ZQ, F-G: QP, H: CP).

2

at 325 °C and 350 °C, respectively. A quality control (QC) sample, comprising a 1 mL mixture of aliquots from each sample solution, was analyzed initially and after every eighth injection to maintain instrument stability throughout the batch analysis.

2.4. HPLC analysis

Separation of the targeted compounds was achieved using a 1260 Infinity II system (Agilent-Tech, California, USA) equipped with a Waters Atlantis® T3 C$_{18}$ column (4.6 × 250 mm, 5 μm). An optimized elution gradient was employed with a composition of acetonitrile (A) and water (B) with the following profile: 0–30-40–55-65 min; 5–25-40–95-95 % A. The HPLC system was set to operate at a column temperature of 28 °C, a flow rate of 0.8 mL/min, a UV detection wavelength of 284 nm, and an injection volume of 5 μL to achieve optimal separation conditions.

The precision, repeatability, and stability of the HPLC method were validated by analyzing six replicates, six parallel samples, and the same sample at eight different time points. Calibration curves were generated by analyzing the reference standards at six known concentrations (N. Muhammad et al., 2018). The single standard to determine multi-components (SSDMC) approach was adopted using naringin as the reference, as previously described (J. Luo et al., 2023). A standard with known concentration was added to an accurately weighed sample to calculate the recovery rate. Limits of Detection (LOD) and Limits of Quantification (LOQ) were computed based on signal-to-noise ratios (S/N) of 3 and 10, respectively (Subhani et al., 2020). The durability of the method was verified by employing three columns across two LC systems.

2.5. TLC analysis

TLC chromatograms were generated using an SP-20E automatic sampler coupled with the Goodlook-1000 TLC imaging system from Kezhe (Shanghai, China). A reference solution at a concentration of 0.5 mg/mL was prepared by dissolving narirutin, hesperidin, neohesperidin, and naringin in methanol. Separate applications of 2 μL of each test and reference solution were made onto the same polyamide film plate, employing a developing agent of acetone and water in a 3:2 (v/v) ratio. After the application and subsequent drying, the plate was sprayed with a 5 % solution of aluminum trichloride in ethanol and allowed to develop to a distance of 8 cm from the line of origin. Examination under ultraviolet light at 365 nm followed for visualization of the plate.

2.6. Antioxidant activity analysis

The scavenging activity against the DPPH radical was evaluated using a modified procedure. Briefly, 3.5 mg of DPPH powder was dissolved in 50 mL of ethanol, and the solution was subjected to ultrasonic extraction for 5 min with adequate shaking to ensure homogeneity. Subsequently, a test solution was prepared by combining of 20 μL of the sample with 600 μL of the DPPH solution, which was further supplemented with methanol to achieve a final volume of 1000 μL. The test solution was thereupon incubated for 30 min in the dark, after which absorbance was recorded at 517 nm using a UV spectrophotometer (Jinghua Tech, Shanghai, China). Methanol served as the internal control. All experiments were conducted in triplicate, and the changes in the components of the reacted solutions were detected using HPLC.

The ABTS scavenging potential of the extracts was assessed in conformity with the instructions accompanying the assay kit. The test solution consisted of 50 μL of the sample solution, 170 μL of ABTS solution, and 20 μL of peroxidase solution. Following a 6-minute incubation period, absorbance at 410 nm was recorded using a microplate detector (Beijing Heng Odd Tech, Beijing, China). Distilled water was employed as the internal control, and the analyses were performed in triplicate.

The DPPH and ABTS radical scavenging activities were calculated using the following formula: Scavenging Activity (%) = (1-Asample)/

Acontrol × 100 %.

2.7. Data analysis

Compound Discoverer 3.3 software facilitated LC-MS data processing, including peak rating and *P*-value computation. The violin plot was constructed using Origin 2022. Compound identification was based on the mzVault, mzCloud, ChemSpider, and Mass List Search databases. SPSS 21 was used to perform the Kruskal Wallis test, and ClogP values were calculated with Chemdraw Ultra 14.0. The HPLC fingerprint was generated using the Similarity Evaluation System for Chromatographic Fingerprint of Traditional Chinese Medicine (Version 2012A). SIMCA 14.1 software was utilized for principal component analysis (PCA), partial least squares discriminant analysis (PLS-DA), and partial least squares regression (PLS-r) analysis. MetaboAnalyst (https://www.metaboanalyst.ca/) was used to conduct the normal distribution test, hierarchical clustering (HCA) analysis, and Pearson correlation coefficient (PCCs) calculations, while the grey relational analysis (GRA) was performed on the SPSS Pro (https://www.spsspro.com).

3. Results and discussion

3.1. UPLC-MS analysis

The PCA score plot demonstrated excellent aggregation of QC samples at the center, indicating instrument stabilization during injections (Fig. S1A). The analysis of all sample data by Compound Discoverer software yielded 14,735 features. Since not all features conformed to a normal distribution, the Kruskal-Wallis test was employed to identify statistical differences among the five groups ($p < 1.0E-07$). Subsequent screening retained 662 features for further analysis. The HCA heatmap, constructed from these 662 differential features, displayed five distinct clusters, each characterized by unique component intervals (Fig. S1B and S2).

Flavonoids, coumarins, alkaloids, and limonoids were the predominant compounds in *Citrus* products (Fig. 2A) (Jiangyi Luo et al., 2023). Flavanone *O*-glycosides displayed typical fragmentation patterns that included continuous sugar loss, glucose cleavage, and Retro Diels-Alder (RDA) cleavage, forming prominent ions at *m/z* 147, 153, and 177 (Fig. 2B) (Yu et al., 2020). The neutral loss of glycosides led to the formation of aglycones such as naringenin (**31**, **70**, **73–74**, **77**), hesperetin (**27**, **43**, **85**, **90**), and isosakuranetin (**57**, **110–111**, **115–116**), with diagnostic ions at *m/z* 273.0763, 303.0869, and 287.0919 [M + H]$^+$, respectively (Tong, Peng, Tong, Guo, & Shi, 2018).

The sugar moieties of flavone *C*-glycosides in *Citrus* are substituted exclusively at the 6- and/or 8-positions, forming fragment ions [M + H–nH$_2$O]$^+$ after a continuous loss of H$_2$O (Duan et al., 2014). The sugar cleavages generated diagnostic ions [M + H–C$_3$H$_6$O$_3$]$^+$ ($^{0, 3}$X) and [M + H–C$_4$H$_8$O$_4$]$^+$ ($^{0, 2}$X) by loss of 90 Da and 120 Da, respectively (Fig. 2C) (A. Singh, Kumar, Bajpai, Reddy, Rameshkumar, & Kumar, 2015). For instance, compound **25** displayed precursor ion [M + H]$^+$ at *m/z* 595.1641 (C$_{27}$H$_{30}$O$_{15}$), which formed product ions at *m/z* 577.1567 [M + H–H$_2$O]$^+$, 559.1456 [M + H–2H$_2$O]$^+$, and 523.1218 [M + H–4H$_2$O]$^+$, along with 505.1121 [M + H–90]$^+$ and 475.1096 [M + H–120]$^+$, consistent with the characteristic ions of vicenin-2 (Tong et al., 2018). Additionally, 6-*C*-glycosides (**39** and **46**) exhibited a higher abundance of the product ion [M + H–H$_2$O]$^+$ compared to the isomeric 8-*C*-glycosides (**34** and **50**) (A. Singh et al., 2015). The retention times (RTs) of flavonoid isomers were predicted by ClogP, with higher ClogP values corresponding to longer RTs (Z. Wang, Li, Chambers, Crane, & Wang, 2021).

Polymethoxyflavones were characterized by diagnostic ions [M + H–nCH$_3$]$^+$, accompanied by fragmentation of CH$_4$, CO, CO$_2$, and H$_2$O. For example, nobiletin (**171**) exhibited a [M + H]$^+$ at *m/z* 403.1388 and product ions at *m/z* 388.1146 [M + H–CH$_3$]$^+$, 373.0910 [M + H–2CH$_3$]$^+$, 355.0814 [M + H–2CH$_3$–H$_2$O]$^+$, and 327.0855 [M +
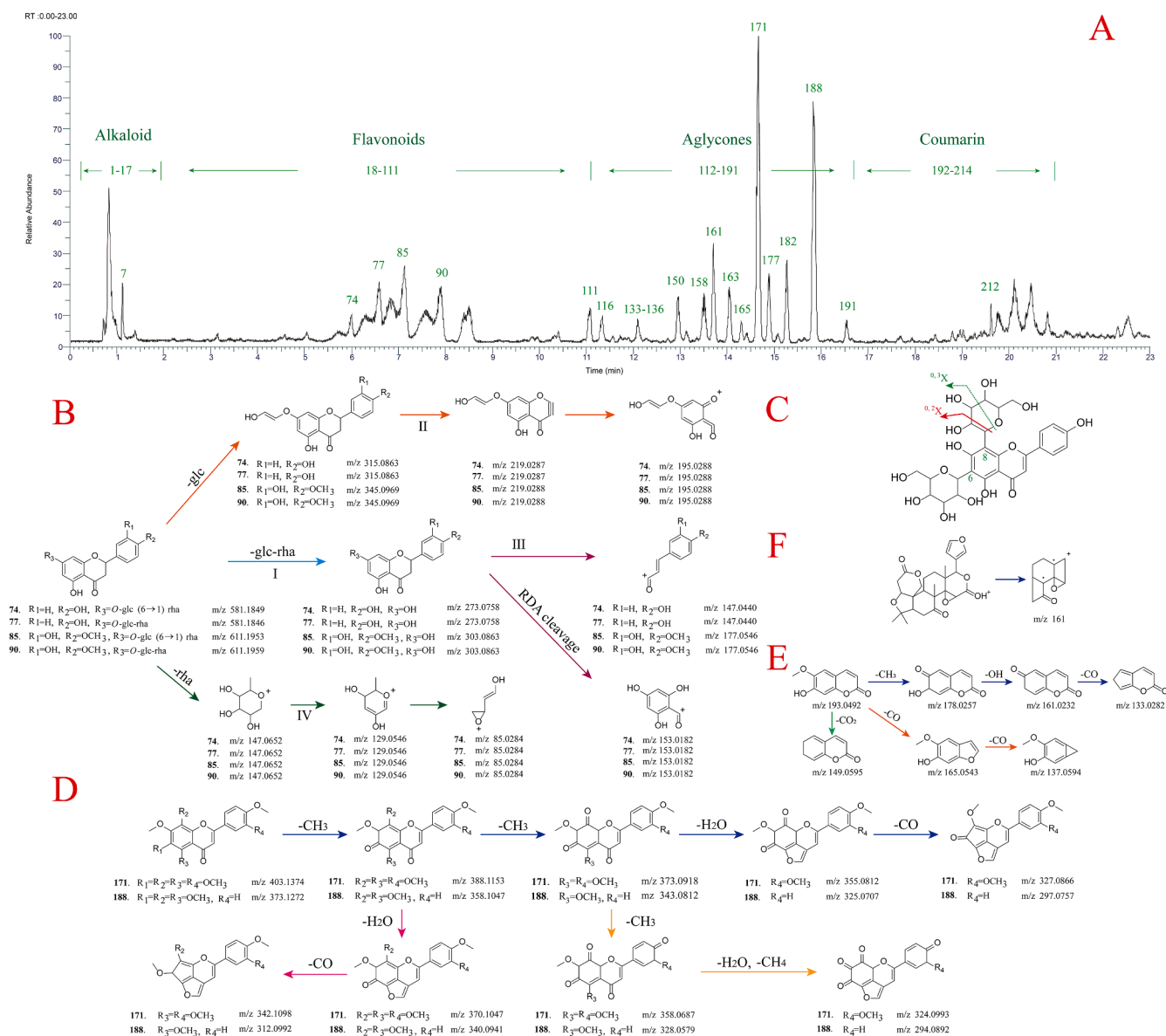
Fig. 2. Total ion chromatogram of QC sample (A) and the proposed fragmentation patterns of flavanone *O*-glycosides (B), flavone *C*-glycosides (C), poly-methoxyflavones (D), coumarins (E), and limonoids (F).

H–2CH$_3$–H$_2$O–CO]$^+$, with the proposed fragmentation pathways illustrated in Fig. 2D (Duan et al., 2014). Coumarins and limonoids were primarily fragmented by the loss of small molecular groups (CH$_3$, CO, OH, CO$_2$, H$_2$O, or CH$_3$COOH), with *m/z* 161.0594 identified as the diagnostic ion for the latter (Fig. 2E-F) (Bai et al., 2018; Yu et al., 2020). From the 662 features, 214 compounds were identified by employing a multi-faceted approach that included database searches in mzVault, mzCloud, ChemSpider, and Mass List Search, analysis of previously reported LC-MS data, and evaluation of proposed fragmentation pathways from six reference standards (Table S2).

Several factors are taken into account when determining peak rating values for chromatographic peaks, encompassing peak quality factors, relative peak area, and coefficient of variance (CV) values. A peak rating threshold of > 0.9 was applied to all samples within each group, resulting in 112 common compounds being screened from the initial 214 identified compounds. An unpaired ANOVA model with Tukey post-hoc test and Benjamini-Hochberg adjustment exposed 59 characteristic compounds that distinguished each sample group based on significant *P*-values (<0.01). Details of these 59 compounds are highlighted in green

in Table S2. The first two principal components represented 49.7 % of 14,735 features, which increased to 78.6 % of 662 features and further to 83.4 % of 59 compounds, signifying an enhanced classification quality (Fig. 3A-C). PLS-DA analysis was subsequently conducted on the 59 compounds, revealing compounds **85** (hesperidin), **90** (neo-hesperidin), **78** (naringeninchalcone), **74** (narirutin), and **77** (naringin) as essential compounds, as reflected by their Variable Importance in Projection (VIP) values exceeding 1.5 (Fig. 3D).

3.2. HPLC analysis

The established method underwent a methodological assessment to ascertain its precision, repeatability, stability, and durability (Table S3), with RSD values of < 2.0 % confirming reliability (Nadeem Muhammad et al., 2022). Fifteen characteristic peaks (**P1**-**P15**) were calibrated for analysis. The principal distinction between the fruit of *C. aurantium* (SCZS and ZQ) and its cultivar Daidai (SCZS-DD and ZQ-DD) was noted in the levels of narirutin and compounds with RTs between 36 and 40 min (Fig. 4A). Narirutin, hesperidin, naringin, neohesperidin, and three
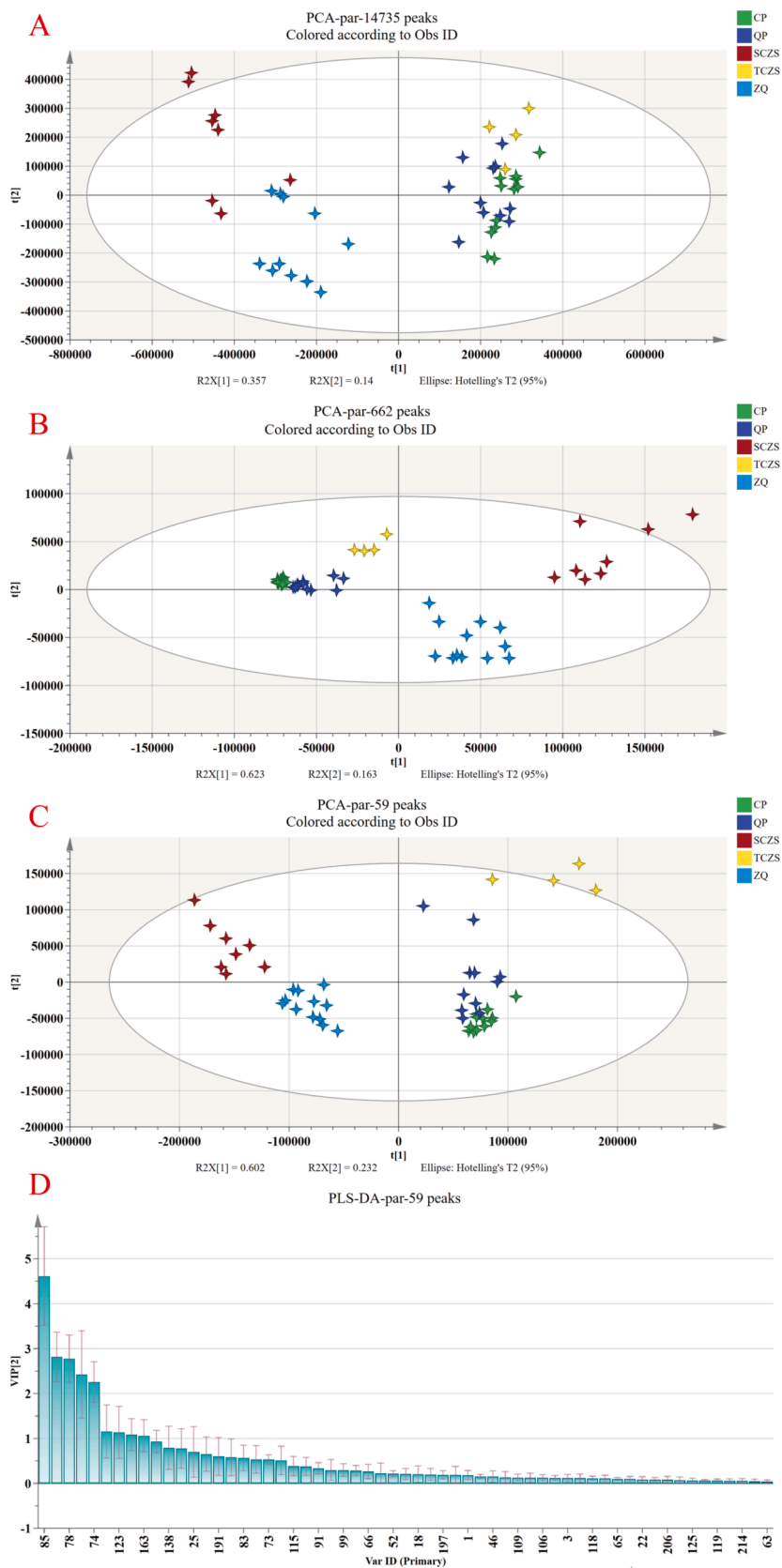
Fig. 3. The PCA score plot of 14,735 features (A), 662 features (B), and 59 compounds (C), and VIP values of 59 compounds (D).
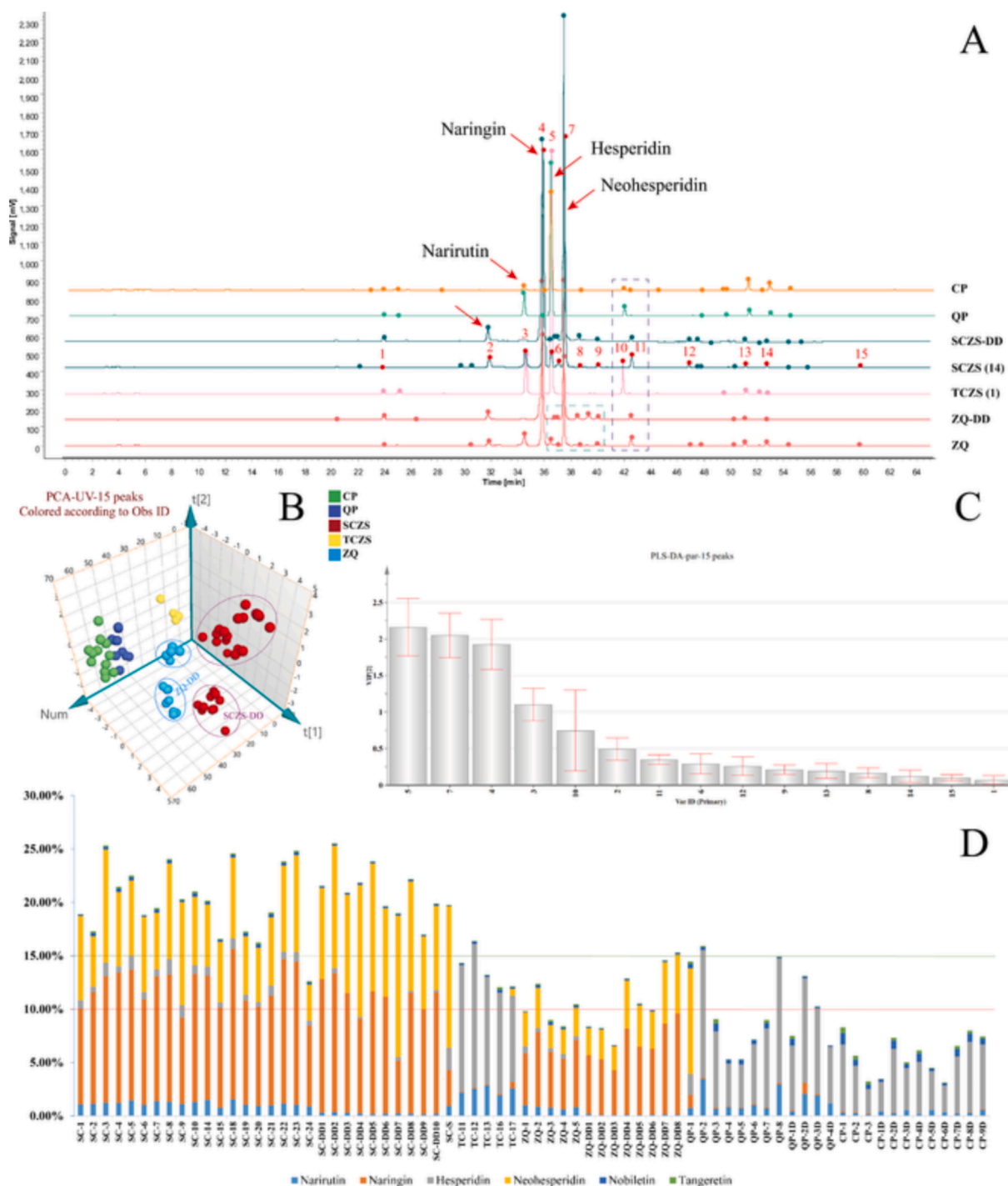
Fig. 4. The comparison of reference fingerprint of citrus by-products (A), PCA score plot (B), VIP values (C) of 15 peaks, and content of the compounds in samples (D).

unknown peaks (**P2**, **P10**, and **P11**), were key in distinguishing SCZS from TCZS, and these compounds were present at lower levels in QP and CP (Fig. 4A). Furthermore, four adulterants were detected through their significantly distinct HPLC chromatograms compared to authentic samples (Fig. S3).

The PCA analysis elucidated the disparities in main components among the various products (Fig. 4B). A Biplot, generated by merging the PCA analysis with a loading score plot, enabled an intuitive assessment of feature contribution to classification. Similar dispersion patterns were noted for TCZS, QP, and CP as for **P5** (hesperidin), **P3** (narirutin), and **P10**, whereas **P4** (naringin), **P7** (neohesperidin), and **P2** were

critical peaks identified in SCZS and ZQ (Fig. S4). The PLS-DA analysis isolated hesperidin, neohesperidin, naringin, and narirutin as crucial components for classification, as denoted by their VIP above 1.0 (Fig. 4C).

The calibration curves for all six compounds demonstrated outstanding linearity, with R^2 values exceeding 0.9991 (Table S4). The recovery rates for these compounds ranged from 95.1 % to 107.7 %, with RSDs less than 1.2 %, showcasing the robustness of the method (Table S5). The response factors for narirutin, hesperidin, neohesperidin, nobiletin, and tangeretin were 1.11, 1.01, 0.73, 1.29, and 0.79, respectively. Notably, no significant differences were observed

between the results obtained from the SSDMC and those obtained using the calibration curve method (Table S6). While SCZS and ZQ contained high levels of naringin (7.56 %-14.10 % in SCZS and 4.20 %-9.49 % in ZQ) and neohesperidin (3.37 %-13.23 % in SCZS and 2.15 %-5.77 % in ZQ), TCZS, QP, and CP were enriched in narirutin (1.93 %-2.84 % in TCZS, 0.44 %-3.46 % in QP, and 0.14 %-0.56 % in CP) and hesperidin (9.49 %-13.44 % in TCZS, 3.98 %-11.93 % in QP, and 2.30 %-6.56 % in CP) (Fig. 4D). As the *C. aurantium* fruit ripened, levels of flavonoid *O*-glycosides (S. Wang et al., 2016), specifically naringin and neo-hesperidin—compounds contributing to the bitterness of citrus fruits—progressively decreased (Tang et al., 2021). The peel of *C. reticulata* displayed a reduction in narirutin and hesperidin content; contrastingly, the levels of polymethoxyflavones, such as nobiletin and tangeretin, exhibited an upward trend.

3.3. TLC analysis

The TLC analysis corroborated the critical components identified through LC-Orbitrap-MS and HPLC analyses, including narirutin, naringin, hesperidin, and neohesperidin, as well as variations in their content. SCZS, distinguishable by its high naringin and neohesperidin levels, contrasted with TCZS, which displayed elevated concentrations of hesperidin and narirutin. Meanwhile, C1, C2, and hesperidin bands facilitated the differentiation between SCZS, ZQ, and ZQ-DD. QP and CP contained low levels of hesperidin and narirutin, respectively (Fig. 5). Taken together, the findings from 72 sample batches were consistent with the aforementioned outcomes (Fig. S5). The optimized TLC approach, compared to previously reported methods (Commission, 2020; Section, 2020; Welfare, 2021), yielded cleaner and clearer bands, detecting additional markers, thereby suggesting broad applicability to citrus by-products and significant potential in authentication processes.

3.4. Antioxidant activity analysis

The DPPH radical scavenging rates for the five groups varied from 10 % to 50 %, with SCZS showing a mean value of 38 %, which was higher than the other groups. Significant scavenging rates against ABTS in the range of 55 %-80 % were observed across all five groups; however, there were notable variances in the data obtained from the ZQ and QP samples (Fig. 6A-B).

The PLS-r analysis correlating 15 characteristic HPLC peaks with DPPH or ABTS scavenging rates was conducted using SIMCA 14.1

software. The VIP scores revealed **P7** (neohesperidin), **P4** (naringin), and **P5** (hesperidin) as significantly related to the DPPH radical scavenging activity, whereas **P13** (nobiletin), **P6**, and **P14** (tangeretin) were recognized as the most critical components for the ABTS scavenging activity (Fig. 6C-D). Compounds with GRA grades above 0.9 were strongly correlated with bioactivity. Specifically, peaks **P1**, **P2**, **P4**, **P7**, **P9**, and **P13** demonstrated a significant impact on the DPPH scavenging activity, while **P1**, **P3**, **P13**, and **P14** were determined to be relevant compounds for the ABTS scavenging activity (Table S7). Under the screening conditions of PCCs exceeding 0.4 and $p < 0.01$, **P2**, **P4**, **P7**, and **P12** had a strong positive correlation with DPPH radical scavenging activity (Table S8). Nonetheless, no characteristic peaks exhibited a strong link with the ABTS scavenging ability (Fig. S6).

Integrating the results from the PLS-r, GRA, and PCCs analyses, compounds **P7** (neohesperidin) and **P4** (naringin) were confirmed as key markers for DPPH scavenging activity (Fig. S7A), which was further substantiated by the online HPLC-DPPH antioxidant assay (Fig. S8). Despite exhibiting higher levels than naringin in the samples, neohesperidin displayed a smaller peak area than naringin after the reaction, indicating its superior contribution to the DPPH scavenging activity, in line with the previously mentioned spectrum-effect relationship results. Of note, **P13** (nobiletin) and **P14** (tangeretin) significantly contributed to ABTS scavenging activity (Fig. S7B).

4. Conclusion

The present study devised a systematic method by integrating UPLC-MS, HPLC, and TLC analyses with antioxidant capacity validation to identify bioactive compounds in five citrus by-products. An in-depth component analysis of these by-products unveiled that citrus fruits typically contain flavonoids, coumarins, alkaloids, and limonoids. Noteworthily, each by-product presented distinctive characteristics regarding the levels of different compounds. For example, QP and CP exhibited relatively lower levels of coumarins compared to the others. Sweet oranges and mandarin oranges possessed higher levels of taste-neutral compounds, such as hesperidin and narirutin. Conversely, sour and bitter oranges were richer in naringin and neohesperidin, contributing to their bitter taste. The levels of these components decreased with the ripening of the fruit. These chemical variances can influence pharmacological activities and therapeutic efficacies, such as antioxidant capacities. Consequently, citrus fruits are utilized for two purposes, based on their harvesting time. The present study validated the
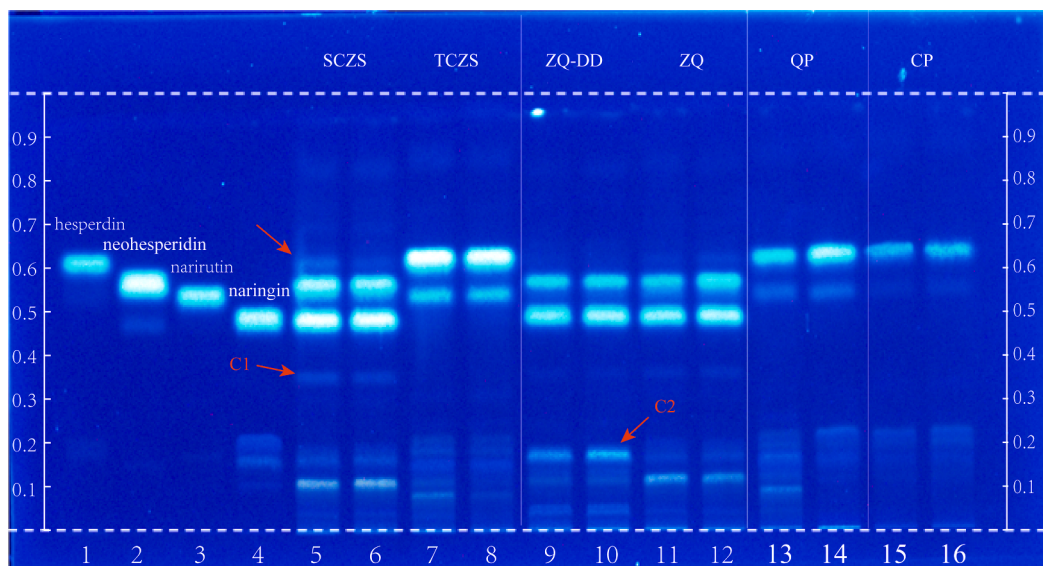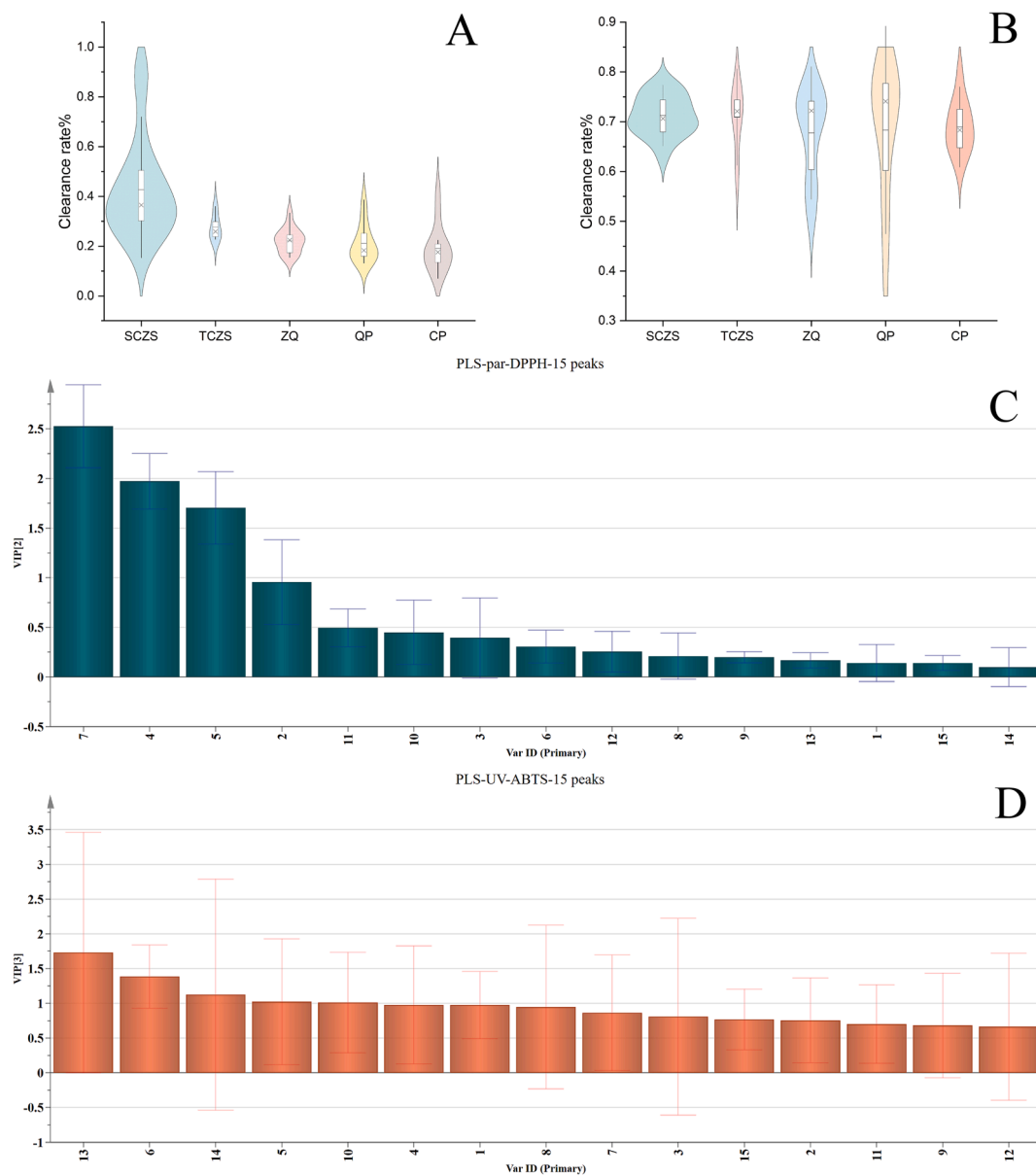

Fig. 5. TLC fingerprint of citrus by-products (1-hesperdin, 2-neohesperdin, 3-narirutin, 4-naringin, 5 ∼ 6-SCZS, 7 ∼ 8-TCZS, 9 ∼ 12-ZQ, 13 ∼ 14-QP, 15 ∼ 16-CP).

Fig. 6. The result of DPPH (A) and ABTS (B) scavenging activities, and VIP value of each peak for DPPH (C) and ABTS (D) scavenging activities.

practicality of the online HPLC assay for assessing antioxidant capacities. Spectrum-effect relationship analysis offered insights into the correlation between antioxidant capacity and active compounds. Furthermore, the current study highlighted the effectiveness of TLC technology in distinguishing citrus by-products following methodological optimization. In summary, this research provides a valuable reference for the authentication and quality control of citrus by-products.

Credit Author Statement

All authors made contributions to this study. Jiangyi Luo was responsible for the planning, design, and editing of the paper. Ling Liang assisted in creating figures, while Lijuan Zhu, Yangfen Fu, and Qinling Xie aided in compiling the literature. Yupei Yang, Sai Jiang, and Yixing Qiu contributed to table preparation. Hanwen Yuan, Shenghuang Chen, and Wei Wang provided corrections, revisions, improvements, and finalization of the manuscript.

Declaration of competing interest

The authors declare that they have no known competing financial interests or personal relationships that could have appeared to influence the work reported in this paper.

Data availability

No data was used for the research described in the article.

Acknowledgments

Appendix A. Supplementary data

Supplementary data to this article can be found online at https://doi.org/10.1016/j.fochx.2023.101010.

References

Bai, Y., Zheng, Y., Pang, W., Peng, W., Wu, H., Yao, H., … Su, W. (2018). Identification and Comparison of Constituents of Aurantii Fructus and Aurantii Fructus Immaturus by UFLC-DAD-Triple TOF-MS/MS. *Molecules, 23*(4). https://doi.org/10.3390/molecules23040803

Commission, C. P. (2020). *Pharmacopoeia of the People's Republic of China*. Beijing: People's Medical Publishing House.

Costanzo, G., Vitale, E., Iesce, M. R., Naviglio, D., Amoresano, A., Fontanarosa, C., … Arena, C. (2022). Antioxidant properties of pulp, peel and seeds of phlegrean mandarin (Citrus reticulata Blanco) at different stages of fruit ripening. *Antioxidants (Basel), 11*(2). https://doi.org/10.3390/antiox11020187

Czech, A., Malik, A., Sosnowska, B., & Domaradzki, P. (2021). Bioactive substances, heavy metals, and antioxidant activity in whole fruit, peel, and pulp of citrus fruits. *Int J Food Sci, 2021*, 6662259. https://doi.org/10.1155/2021/6662259

Duan, L., Guo, L., Liu, K., Liu, E. H., & Li, P. (2014). Characterization and classification of seven citrus herbs by liquid chromatography-quadrupole time-of-flight mass spectrometry and genetic algorithm optimized support vector machines. *J Chromatogr A, 1339*, 118–127. https://doi.org/10.1016/j.chroma.2014.02.091

Farag, M. A., Abib, B., Ayad, L., & Khattab, A. R. (2020). Sweet and bitter oranges: An updated comparative review of their bioactives, nutrition, food quality, therapeutic merits and biowaste valorization practices. *Food Chem, 331*, Article 127306. https://doi.org/10.1016/j.foodchem.2020.127306

Liang, S., Zhang, J., Liu, Y., Wen, Z., Liu, X., Dang, F., … Wu, H. (2022). Study on flavonoids and bioactivity features of pericarp of Citrus reticulata "Chachi" at different harvest periods. *Plants (Basel), 11*(23). https://doi.org/10.3390/plants11233390

Luo, J., Yuan, H., Liang, L., Xie, Q., Jiang, S., Fu, Y., … Wang, W. (2023). An integrated strategy for quality control of the multi-origins herb medicine of Gentianae Macrophyllae Radix based on UPLC-Orbitrap-MS/MS and HPLC-DAD. *RSC Advances, 13*(13), 8847–8862. https://doi.org/10.1039/d2ra07591a

Luo, J., Yuan, H., Mao, L., Wu, J., Jiang, S., Yang, Y., … Wang, W. (2023). The young fruit of Citrus aurantium L. or Citrus sinensis Osbeck as a natural health food: A deep insight into the scientific evidence of its health benefits. *Arabian Journal of Chemistry, 16*(5). https://doi.org/10.1016/j.arabjc.2023.104681

Muhammad, N., Hussian, I., Ali, A., Hussain, T., Intisar, A., Ul Haq, I., … Zhu, Y. (2022). A comprehensive review of liquid chromatography hyphenated to post-column photoinduced fluorescence detection system for determination of analytes. *Arabian Journal of Chemistry, 15*(9). https://doi.org/10.1016/j.arabjc.2022.104091

Muhammad, N., Wang, F., Subhani, Q., Zhao, Q., Qadir, M. A., Cui, H., & Zhu, Y. (2018). Comprehensive two-dimensional ion chromatography (2D-IC) coupled to a post-column photochemical fluorescence detection system for determination of neonicotinoids (imidacloprid and clothianidin) in food samples. *RSC Advances, 8*(17), 9277–9286. https://doi.org/10.1039/c7ra12555k

H.K.C.M.M.S. Section. (2020). *Hong Kong Chinese Materia Medica Standards*. Hong Kong Special Administrative Region, The People's Republic of China: Department of Health.

Singh, A., Kumar, S., Bajpai, V., Reddy, T. J., Rameshkumar, K. B., & Kumar, B. (2015). Structural characterization of flavonoid C- and O-glycosides in an extract of Adhatoda vasica leaves by liquid chromatography with quadrupole time-of-flight mass spectrometry. *Rapid Communications in Mass Spectrometry, 29*(12), 1095–1106. https://doi.org/10.1002/rcm.7202

Singh, B., Singh, J. P., Kaur, A., & Yadav, M. P. (2021). Insights into the chemical composition and bioactivities of citrus peel essential oils. *Food Research International, 143*, Article 110231. https://doi.org/10.1016/j.foodres.2021.110231

Subhani, Q., Muhammad, N., Huang, Z., Asif, M., Hussain, I., Zahid, M., … Guo, D. (2020). Simultaneous determination of acetamiprid and 6-chloronicotinic acid in environmental samples by using ion chromatography hyphenated to online photoinduced fluorescence detector. *Journal of Separation Science, 43*(20), 3921–3930. https://doi.org/10.1002/jssc.202000635

Sun, Y., Wang, J., Gu, S., Liu, Z., Zhang, Y., & Zhang, X. (2010). Simultaneous determination of flavonoids in different parts of Citrus reticulata 'Chachi' fruit by high performance liquid chromatography-photodiode array detection. *Molecules, 15*(8), 5378–5388. https://doi.org/10.3390/molecules15085378

Tang, Q., Zhang, R., Zhou, J., Zhao, K., Lu, Y., Zheng, Y., … He, Y. (2021). The levels of bioactive ingredients in Citrus aurantium L. at different harvest periods and antioxidant effects on H(2) O(2) -induced RIN-m5F cells. *Journal of the Science of Food and Agriculture, 101*(4), 1479–1490. https://doi.org/10.1002/jsfa.10761

Tian, F., He, X. F., Sun, J., Liu, X. D., Zhang, Y., Cao, H., … Ma, Z. (2020). Simultaneous quantitative analysis of nine constituents in six Chinese medicinal materials from Citrus genus by high-performance liquid chromatography and high-resolution mass spectrometry combined with chemometric methods. *Journal of Separation Science, 43*(4), 736–747. https://doi.org/10.1002/jssc.201901033

Tocmo, R., Pena-Fronteras, J., Calumba, K. F., Mendoza, M., & Johnson, J. J. (2020). Valorization of pomelo (Citrus grandis Osbeck) peel: A review of current utilization, phytochemistry, bioactivities, and mechanisms of action. *Comprehensive Reviews in Food Science and Food Safety, 19*(4), 1969–2012. https://doi.org/10.1111/1541-4337.12561

Tong, R., Peng, M., Tong, C., Guo, K., & Shi, S. (2018). Online extraction-high performance liquid chromatography-diode array detector-quadrupole time-of-flight tandem mass spectrometry for rapid flavonoid profiling of Fructus aurantii immaturus. *Journal of Chromatography B: Analytical Technologies in the Biomedical and Life Sciences, 1077–1078*, 1–6. https://doi.org/10.1016/j.jchromb.2018.01.031

Wang, S., Tu, H., Wan, J., Chen, W., Liu, X., Luo, J., … Zhang, H. (2016). Spatio-temporal distribution and natural variation of metabolites in citrus fruits. *Food Chemistry, 199*, 8–17. https://doi.org/10.1016/j.foodchem.2015.11.113

Wang, Y., Qian, J., Cao, J., Wang, D., Liu, C., Yang, R., … Sun, C. (2017). Antioxidant capacity, anticancer ability and flavonoids composition of 35 citrus (Citrus reticulata Blanco) Varieties. *Molecules, 22*(7). https://doi.org/10.3390/molecules22071114

Wang, Z., Li, J., Chambers, A., Crane, J., & Wang, Y. (2021). Rapid structure-based annotation and profiling of dihydrochalcones in star fruit (Averrhoa carambola) using UHPLC/Q-Orbitrap-MS and molecular networking. *Journal of Agricultural and Food Chemistry, 69*(1), 555–567. https://doi.org/10.1021/acs.jafc.0c07362

Welfare, M.o. H.a. (2021). *Taiwan Herbal Pharmacopeia*. Taiwan: Taiwan Herbal Pharmacopeia Commission.

Xie, Z. W. (1991). Research on duration and changes of Zhi Shi and Zhi Qiao as ancient and present drugs. *Chinese Journal of Integrative Medicine on Cardio-Cerebrovascular Disease, 1*, 19–22.

Yu, L., Chen, M., Liu, J., Huang, X., He, W., Qing, Z., & Zeng, J. (2020). Systematic detection and identification of bioactive ingredients from Citrus aurantium L. var. amara Using HPLC-Q-TOF-MS combined with a screening method. *Molecules, 25*(2). https://doi.org/10.3390/molecules25020357

Zhao, Y. L., Yang, X. W., Wu, B. F., Shang, J. H., Liu, Y. P., Zhi, D., & Luo, X. D. (2019). Anti-inflammatory effect of pomelo peel and its bioactive coumarins. *Journal of Agricultural and Food Chemistry, 67*(32), 8810–8818. https://doi.org/10.1021/acs.jafc.9b02511